



**HAL**  
open science

## Introducing Meta-models for a More Efficient Hazard Mitigation Strategy with Rockfall Protection Barriers

D. Toe, A. Mentani, L Govoni, Franck Bourrier, G. Gottardi, Stéphane Lambert

► **To cite this version:**

D. Toe, A. Mentani, L Govoni, Franck Bourrier, G. Gottardi, et al.. Introducing Meta-models for a More Efficient Hazard Mitigation Strategy with Rockfall Protection Barriers. *Rock Mechanics and Rock Engineering*, 2018, 51 (4), pp.1097 - 1109. 10.1007/s00603-017-1394-9 . hal-01893620

**HAL Id: hal-01893620**

**<https://hal.science/hal-01893620v1>**

Submitted on 12 Oct 2018

**HAL** is a multi-disciplinary open access archive for the deposit and dissemination of scientific research documents, whether they are published or not. The documents may come from teaching and research institutions in France or abroad, or from public or private research centers.

L'archive ouverte pluridisciplinaire **HAL**, est destinée au dépôt et à la diffusion de documents scientifiques de niveau recherche, publiés ou non, émanant des établissements d'enseignement et de recherche français ou étrangers, des laboratoires publics ou privés.



1 intercepting rock blocks on their route down to the elements at risk. Barriers are typically made  
2 of different metallic components including posts, net, cables and other connecting components  
3 which makes their mechanical response very complex to predict.

4 As for other passive rockfall protection structures, the design of barriers, as well as the defini-  
5 tion of the optimum protection strategy for a given site, relies on trajectory simulation results. In  
6 particular, stochastic trajectory simulation models provide statistics associated to the rock blocks  
7 paths along the slope as well as their reach probability. The design aims at reducing the lat-  
8 ter down to a targeted value while considering the former. More precisely, relevant statistical  
9 descriptors associated to the blocks passing heights and kinetic energies are considered for deter-  
10 mining the required protective structure characteristics in terms of interception height and kinetic  
11 energy absorption capacity respectively (Lambert et al., 2013). In practice, the barrier design for  
12 a given site is mainly based on the comparison of the statistical descriptor of the block kinetic en-  
13 ergy barrier nominal capacity. This capacity is often obtained following the European guideline  
14 ETAG 027 (EOTA, 2013), which provides detailed indications on how to test and assess the per-  
15 formance of a barrier and to obtain the CE marking. Nevertheless, the impact conditions in such  
16 test, which essentially consist in an impact in the center of a 3-spans barrier by a block without  
17 any rotation, can be considered not representative of the wide variety of impact loading cases as  
18 resulting from the interception of blocks on-site. This issue has been long debated over the last  
19 ten years and several research works have suggested that a test in such conditions may not be  
20 the most critical, as it neglects the effects of parameters such as the impact point location or the  
21 incident angle of the block trajectory (Cazzani et al., 2002; Cantarelli et al., 2008; Lambert et al.,  
22 2009; Chanut et al., 2015). This suggests that current design approaches might be inadequate in  
23 accounting for the global ability of barriers in arresting the blocks, considering all the possible  
24 trajectories.

25 Improving the design of barriers as well as assessing their efficiency in reducing the hazard  
26 at the elements at risk requires better accounting for their actual mechanical response to blocks  
27 impacts. This may be undertaken making use of suitable numerical tool, among the various ones  
28 that have been developed over the last 20 years, with increasing complexity with either finite  
29 or discrete element models (FEM or DEM resp.) (Nicot et al., 2001; Volkwein, A., 2005; Got-  
30 tardi and Govoni, 2010; de Miranda et al., 2010; Bertrand et al., 2012; Gentilini et al., 2012,  
31 2013; Escallòn et al., 2014; de Miranda et al., 2015; Bourrier et al., 2015; Mentani et al., 2015;

1 Coulibaly et al., 2017). Validation by real scale experiments proved these models to be rather ac-  
2 curate. Nevertheless, a relatively high computational cost limits their use in view of investigating  
3 the response of barriers varying many parameters, either concerning the structure or the impact  
4 conditions.

5 A promising alternative of accounting for the mechanical response of barriers, for both de-  
6 sign and hazard reduction assessment purposes, consists in using meta-models. Such approach  
7 proposes surrogate models, so called meta-models, of more complex mechanical models, em-  
8 bedding their complexity but are more efficient in terms of computational time (Sudret, 2008;  
9 Blatman and Sudret, 2010; Mollon et al., 2011). In the context of rockfall protection structures,  
10 the surrogate models are computationally cost-effective tools dedicated to statistical analysis  
11 of the structure response to varying impact conditions. Meta-models are widely used in civil  
12 engineering (Jin et al., 2001; Farhang-mehr and Azarm, 2005; Gonzalez-Perez and Henderson-  
13 Sellers, 2008; Toe et al., 2017). Application in the field of rockfall protection structures was  
14 first considered by Bourrier et al. (2015) with the aim of investigating the failure occurrence of a  
15 barrier via a performance function and then by Mentani et al. (2016).

16 This article proposes the use of meta-modelling approaches for improving the design of pas-  
17 sive rockfall protection structures with a specific focus on a barrier intended for low kinetic  
18 energies frequently encountered in the Alpine arc. This barrier type features an interception  
19 structure made of an hexagonal wire mesh supported by longitudinal cables passing through  
20 steel posts. A finite element (FE), three-dimensional, non-linear model of the barrier has been  
21 developed and subjected to impact simulations by varying simultaneously 6 impact parameters  
22 over a wide and a comparatively narrower range. The results of the analyses provides a thorough  
23 insight of the protection barrier behaviour in terms of failure mechanisms and enables to explore  
24 comprehensively its effect on the energy possessed by the impacting block. Meta-models of the  
25 barrier response in terms of block arrest and block kinetic energy reduction have been developed,  
26 considering two sets of impact condition parameters. The first set has been defined based on the  
27 widest possible range for each parameter. The second set has been adapted to the barrier capacity  
28 evaluated in standard conditions.

29 The article is organised as follows. In the first section, details of the FE models and FE  
30 analyses are given and results are discussed in terms of block-structure interaction, revealing  
31 the complexity of the barrier response to impact. In the second section, the development of

1 meta-models of the barrier response is detailed. Then, the meta-model results are presented and  
 2 discussed in terms of accuracy. The discussion addresses the influence of the parameter ranges  
 3 on the meta-models accuracy, the benefits in using these meta-models compared to current design  
 4 approaches, and their application to real cases.

## 5 2. Finite element modelling of a cable-net barrier

6 This section provides the details of the finite element (FE) modelling of a cable-net barrier,  
 7 developed using the commercial code Abaqus (Abaqus, 2013). For this barrier type, the intercep-  
 8 tion structure is made of longitudinal cables, connected to steel posts fully restrained at the base.  
 9 In general, this structure type is also provided with a secondary hexagonal meshwork fastened  
 10 to the longitudinal cables. Although widely used, information on the response to impact of this  
 11 barrier type are scarce. The results of the FE analyses then offer a new insight on the barrier  
 12 mechanical behaviour, while providing the necessary base to the development of a meta-model  
 13 of the block-barrier interaction.

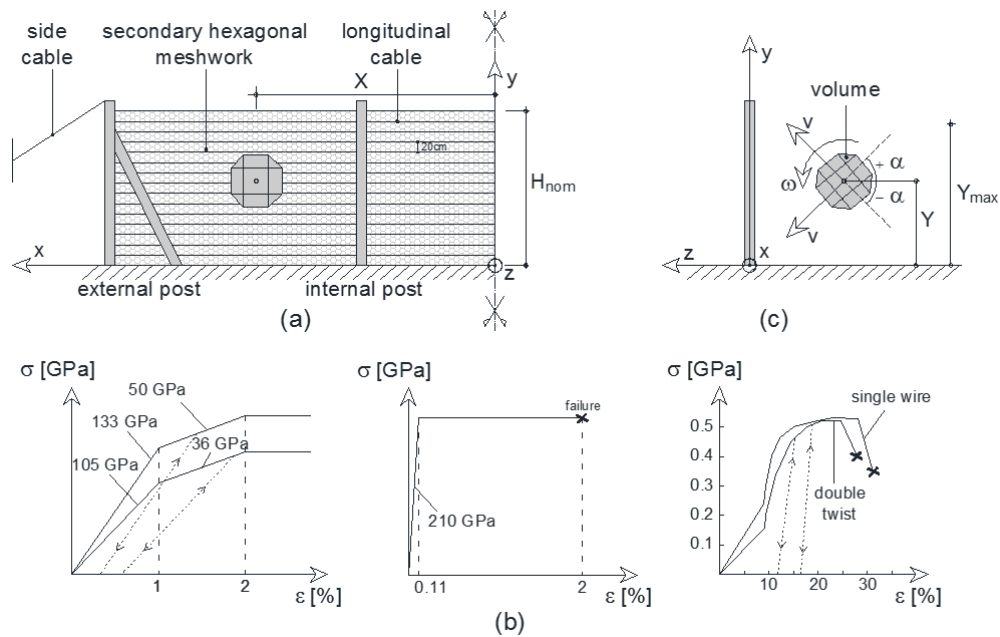


Fig. 1. Geometry and impact conditions for the cable-net protection barrier: a) back view, b) stress-strain behaviour of cables, posts and net and c) side view.

## 1 2.1. FE model

2 As described in Fig. 1a, the study considers a three spans, 5 m spaced, cable-net barrier  
3 of 3.2 m nominal height. Longitudinal cables, 12 mm in diameter, pass through the internal  
4 posts (IPE 200) and are knotted to the external posts (IPE 300), connected to the ground by  
5 side cables of 18 mm diameter. A secondary meshwork, made of a double twisted hexagonal  
6 mesh is connected to the top and bottom longitudinal cables with steel wires. The FE model  
7 of the barrier is three-dimensional and made of one-dimensional elements, whose behaviour  
8 is governed by elasto-plastic constitutive laws. The mechanical response of the barrier elements  
9 was described based on available results of laboratory tests in de Miranda et al. (2015). Particular  
10 attention was devoted to model the behaviour of the wires within the hexagonal mesh, following  
11 data of experiments carried out on mesh portions (Mentani et al., 2015; Thoeni et al., 2013). A  
12 representative scheme of the stress-strain curve for each structural element is given in Fig. 1b,  
13 where the relevant model parameters are also inserted. As depicted, the posts behave following  
14 an elastic-perfectly-plastic law up to a failure limit, cables harden in the plastic phase and may  
15 undergo indefinite deformations once a second yielding threshold is attained and mesh wires  
16 soften prior to fail.

## 17 2.2. FE simulations and results

18 The barrier model was subjected to non-linear dynamic simulations. According to the ref-  
19 erence system and notation introduced in Fig. 1, simulation were carried out, by impacting the  
20 barrier model with a prismatic test block of known volume  $V$ ; at a position of coordinates  $X$  and  
21  $Y$ ; with an incident angle  $\alpha$ ; a translational velocity  $v$ ; and a rotational velocity  $\omega$ .

22  
23 The first simulations were performed in accordance to the procedure described in the Annex  
24 A of ETAG 027 (EOTA, 2013), to provide the cable-net barrier model with a reference capacity  
25 evaluated in standard conditions. In these simulations a translational velocity of 25 m/s and  
26 no rotational velocity were considered. The maximum block mass for which all the Guideline  
27 requirement were fulfilled, was found equal to 640 kg, yielding a reference capacity of 200 kJ  
28 for the cable net barrier. Further analyses were then run to provide the data necessary to the  
29 development of meta-models of the barrier response. To this purpose, parameters related to the  
30 block were varied. Tab. 1 collects these parameters along with their variation ranges, according

Table 1: Input parameters for loading conditions.

Input parameter	unit	Wide Range	Narrow Range
		( <i>WR</i> ) min-max	( <i>NR</i> ) min-max
Translational velocity, $v$	$m/s$	5 - 40	5 - 22.5
Rotational velocity, $\omega$	$rad/s$	0 - 35	0 - 35
Volume of the block, $V$	$m^3$	0.03 - 4	0.03 - 2.5
Incident angle, $\alpha$	$deg$	-60 - 60	-60 - 60
Impact position, $X$	$m$	0 - 7.5	0 - 7.5
Impact position, $Y$	$m$	1 - 2.5	1 - 2.5

1 to the notation introduced in Fig. 1. As indicated in this table, two sets of parameters with  
2 different ranges were considered in this study for generating virtual test programmes: a wide  
3 range set (WR) and a narrow range set (NR) .

4 The wide range (WR) set was considered in agreement with possible output of rockfall tra-  
5 jectory simulations and results of field tests (Bourrier et al., 2009a; Toe et al., 2017). As it is  
6 observed in Tab. 1, a freeboard on the barrier top was inserted, to avoid direct impacts of blocks  
7 on the top cable. A total of 280 simulations were carried out using combinations of the input  
8 parameters. The programme of tests resulted from a Latin-Hypercube sampling, assuming a uni-  
9 form distribution of values within the parameter ranges (Sacks et al., 1989; Fang et al., 2005).

10

11 The results of this set of simulations provided new evidence of the barrier response consid-  
12 ering a wide variety of realistic loading conditions. In particular, four types of block-barrier  
13 interactions were observed, which can be described as follows: i) the block is arrested by the  
14 barrier; ii) the block passes the barrier by rolling over it; iii) the block passes the barrier as a  
15 result of the perforation of the secondary hexagonal meshwork; iv) the block passed the barrier  
16 as a result of the failure of the whole structure.

17

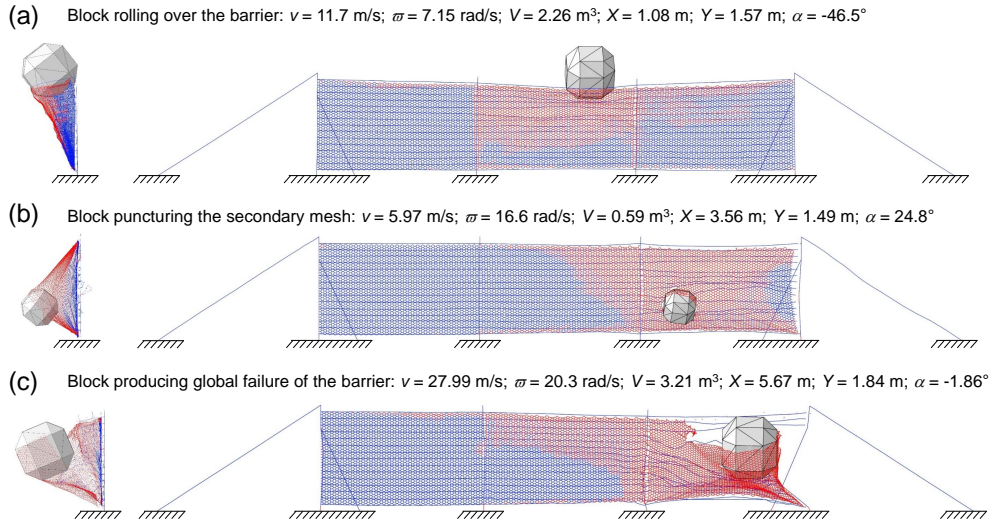
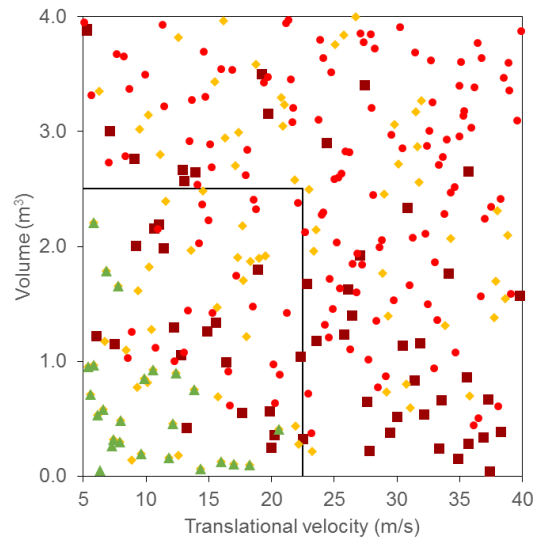


Fig. 2. Block-barrier interaction mechanisms: a) block rolling over; b) mesh perforation and c) global failure.

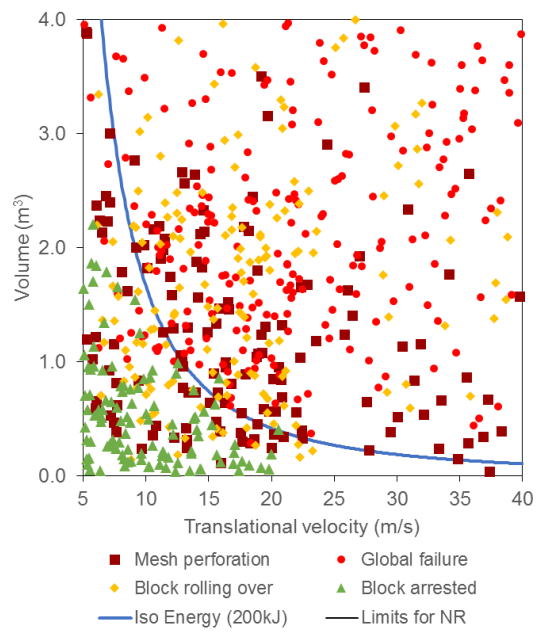
1 Fig. 2 illustrates the front and side views of the deformed barrier through the last instants of  
 2 three selected impact simulations, where the elements which have entered the plastic domain are  
 3 coloured in red. In all these FE tests, the barrier resulted unable to stop the impacting block. In  
 4 particular, Fig. 2a provides an example of the rolling over mechanism, with the block overcom-  
 5 ing the barrier, Fig. 2b depicts the barrier failing due to the perforation of the hexagonal net at a  
 6 side span. Finally, global failure of the barrier is shown in Fig. 2c, with clearly visible formation  
 7 of plastic hinges at one external post, detachment of longitudinal cables and ruptures within the  
 8 secondary meshwork.

9  
 10 In Fig. 3a, the results of the simulations are grouped on the block translational velocity -  
 11 block volume plane, using symbols according to the observed block-barrier interaction mecha-  
 12 nism. Over the 280 simulations, the barrier succeeded in stopping the block in 26 cases. In 254  
 13 cases the barrier failed to stop the block: in 65 cases due to the block rolling over mechanism, in  
 14 57 cases due to mesh perforation and in 132 cases due to global failure. This low barrier success  
 15 ratio is associated to the large ranges considered, without any restriction related to the capacities  
 16 of the barrier. In fact, the points relevant to arrested blocks are characterized by velocities lower  
 17 than 22.5 m/s and by block volumes smaller than 2.5 m<sup>3</sup>.





(a)



(b)

Fig. 3. Results of the analyses on the translational velocity - volume plane: a) wide range and b) wide range and narrow range.

1 A further set of 280 simulations was then performed to obtain more information on the barrier  
2 response within these threshold values, and thus supplying more data for the development of a  
3 meta-model of the barrier ability to arrest a block. In these new FE tests, the translational velocity  
4 and volume were varied within this comparatively narrower range, according to the limit value  
5 indicated in Table 1. As for the wide range, the virtual test programme was designed based on  
6 the Latin-Hypercube sampling procedure.

7 Over the 280 simulations, the barrier succeeded to stop the block in 61 cases. In 219 cases the  
8 barrier failed to stop the block : in 78 cases due to the block rolling over mechanism, in 66 cases  
9 due to mesh perforation and in 75 cases due to global failure.

10 Fig. 3b gather the 560 simulation results from the analyses conducted considering the narrow  
11 and wide range sets. The locus of kinetic energy equal to the determined reference capacity (iso-  
12 energy line at 200 kJ), is also inserted in Fig. 3b. The vast majority of the points corresponding to  
13 the arrested blocks falls below this line. However, cases of barrier failures in arresting the block  
14 are also found below this line. On total, the ratio of observed failure cases to the total number  
15 of cases below this line is as high as 52%. This comment holds for moderate block volumes and  
16 velocities. Indeed, restricting the analysis to cases where the block size is less than 1/3 the barrier  
17 height (thus to block volumes less than  $0.7 \text{ m}^3$  and as suggested by ETAG 027 (EOTA, 2013)),  
18 this ratio equals 33.7%. This suggests that the use of a unique reference capacity value might be  
19 unconservative for this barrier.

20

### 21 2.3. *Effects of the impact parameters on the barrier response*

22 Fig. 4 illustrates the influence of the other impact parameters on the barrier response : the  
23 incident angle (Fig. 4a), the rotational velocity (Fig. 4b), the impact position (Fig. 4c - 4d). For  
24 negative values of incident angle (upward trajectory), the rolling over mechanism is the prevail-  
25 ing block-barrier interaction mode (Fig. 4a). On the velocity plane, although symbols related to  
26 arrested blocks tend to concentrate in the area close to the origin, several points also prove the  
27 ability of the barrier to stop impacting blocks with high rotational velocities, up to 35 rad/sec  
28 (Fig. 4b). As shown in Fig. 4c, the points relevant to the general failure mechanism tend to  
29 concentrate close to the posts, whose location is highlighted with two hatched areas along the  
30 y-axis (position X in Fig. 1). This is particularly clear for translational velocities less than 20  
31 *m/s* and general failures are observed at velocities down to 5 *m/s*.

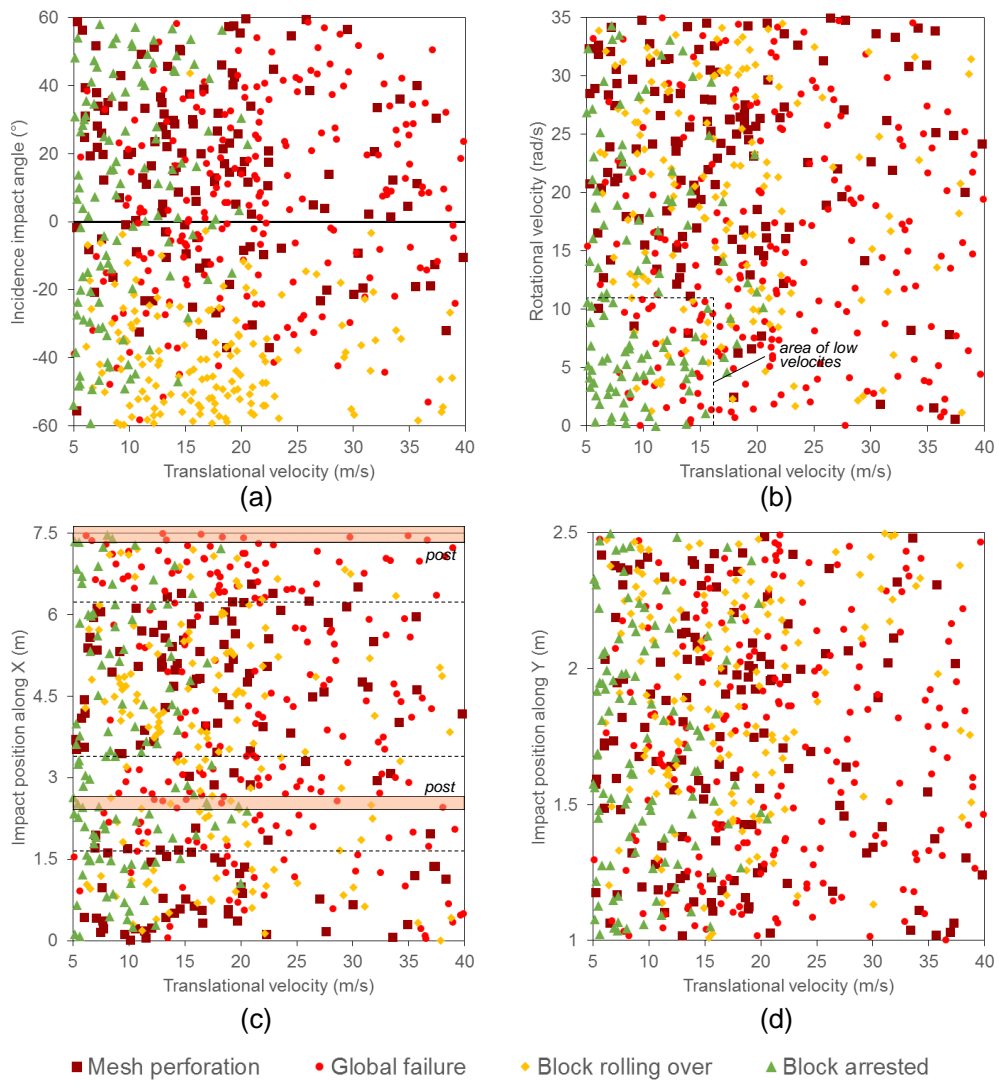


Fig. 4. Results of the analyses as a function of: a) incident impact angle, b) rotational velocity, c) and d) impact position.

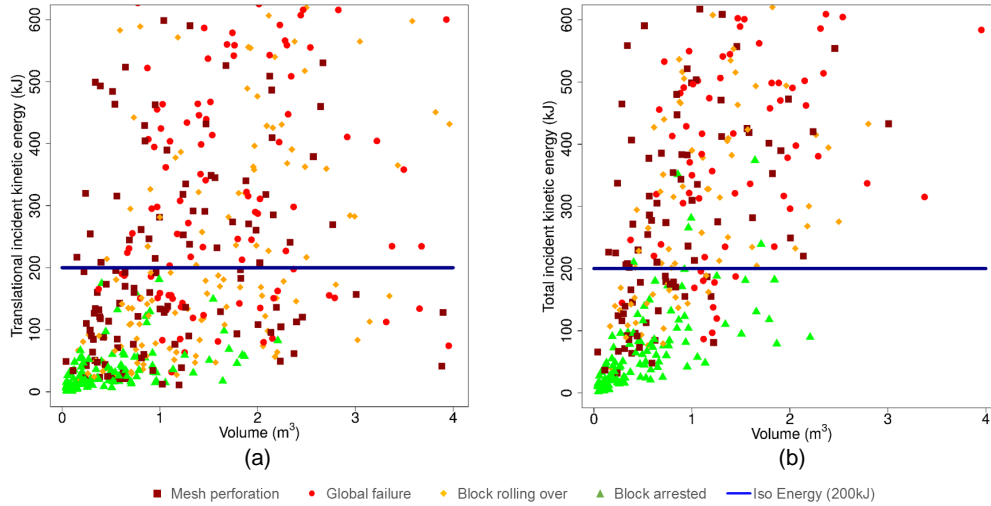


Fig. 5. Results of the analyses as a function of: a) incident impact angle, b) rotational velocity, c) and d) impact position.

1 The influence of the impact position of the block along the y-axis is depicted in Fig. 4d. As it  
 2 is observed, high values of block velocity and position tend to result in a rolling over mecha-  
 3 nism, whereas no significant effects of the position parameter is observed on the barrier ability  
 4 of arresting the block, which remains prevalently driven by the block speed. This is also due to  
 5 the considered freeboard introducing a threshold in the impact height with respect to the barrier  
 6 height.

7 In Fig. 5, the results of the simulations are plotted on the volume-kinetic energy plane up  
 8 to 600 kJ and compared with the iso-energy line. In Fig. 5a the kinetic energy is computed  
 9 by considering the sole contribution of the translational component, while in Fig. 5b the total  
 10 kinetic energy is used, accounting for both the translational and the rotational kinetic energies.  
 11 Comparison shows that, although the upward shifting of the data points from Fig. 5a to Fig.  
 12 5b produces a migration of some arrested block points above the nominal energy line, there are  
 13 still several cases below the line, in which the barrier failed in arresting the block, due to mesh  
 14 perforation, global failure and block rolling over mechanisms.

15

16 Overall, the results show a strong dependency of the barrier response to the impact condi-  
 17 tions. Analysis of the data also showed that, although some trends could be observed, a clear

1 correlation between input parameters and relevant block-barrier interaction mechanisms could  
2 not be established with certainty. These results bring to light the shortcomings of determinis-  
3 tic approaches based on a single impact assessment test, towards the evaluation of a structure  
4 effectiveness, as not adequately accounting for the impact conditions. This crucial aspect can  
5 be more successfully accommodated by reliability probabilistic approaches, through the use of  
6 meta-models which allow for the prediction of the barrier response as a function of the impact  
7 conditions, as described in the following sections.

### 8 **3. The meta-modeling approach**

9 This section provides the essential details of the meta-modelling strategy used in this study.  
10 Meta-models can be defined in this context as mathematical operators describing the response  
11 envelop of a given structure, by considering a large number of variables. With reference to a rock-  
12 fall protection structure, a meta-model can be developed from an optimized number of numerical  
13 simulations, performed using a detailed numerical model of the protection work, allowing for  
14 the prediction of its response to any set of variables, without running extra simulations. Due to  
15 its mathematical structure and computational cost-effectiveness, a meta-model can be integrated  
16 into probabilistic rockfall trajectory models rather easily.

17 Within the context of rockfall hazard assessment, it is important for a meta-model to capture  
18 with accuracy the effects of the structure on the falling block in terms of trajectory and post-  
19 impact kinetic energy. In the light of these general observations, this study focuses on two  
20 essential and correlated aspects of the block-barrier interaction, which are the barrier ability  
21 to arrest a block and, in case of failure, the block post-impact kinetic energy. To the scope,  
22 two different meta-models were developed for these two aspects using classical meta-modeling  
23 techniques.

24 The first meta-model is concerned with two classes: success and failure in arresting the block.  
25 Under the first class, referred to as  $B_{Succ}$ , the arrested block cases are grouped, while the passing  
26 block cases are found to the second class,  $B_{Fail}$ . As dealing with two classes, a Support Vector  
27 Machine (SVM), was used for creating the meta-model (Brereton and Lloyd, 2010; Kausar et al.,  
28 2011). The second meta-model was developed with reference to the  $B_{Fail}$  cases with the aim  
29 to predict the block kinetic energy reduction due to the block-barrier interaction. The value of  
30 energy reduction is given as the difference between the total (translational plus rotational) kinetic

1 energy posses by the block just prior to the impact and the total kinetic energy possessed by the  
2 block just after the impact ( $E_{incident} - E_{out} = E_{RED}$ ). The total kinetic energy was considered in  
3 order to account for possible coupling between translational and rotational velocities, after and  
4 before impact. To this aim, the Kriging method has been used (Kleijnen, 2009; Martin, 2009).  
5 Main features of these two meta-modeling approaches are given in the following sections.

6 The two meta-models were developed using the results of the FE simulations carried out on  
7 the cable-net barrier, by considering the input parameters within wide (*WR*) and narrow (*NR*)  
8 ranges separately. For each range set, a meta-model was created based on the SVM approach to  
9 predict the success or failure of the barrier in stopping the block. Another meta-model was built  
10 based on the Kriging approach to estimate the post-impact total kinetic energy of blocks passing  
11 the barrier. The Kriging approach based meta-model was developed based on the data of the FE  
12 simulations in which the barrier failed in arresting the block.

### 13 3.1. Support Vector Machine

14 The Support Vector Machine (SVM) approach is based on statistical learning theory (Vap-  
15 nik, 1995), and can be used to build a meta-model which can predict the class of an output data.  
16 This method has been used in many different fields of study as for examples remote sensing  
17 (Mountrakis et al., 2011), shape recognition (Ma and Ding, 2002), genomics recognition (Son-  
18 nenburg et al., 2005) and spam detection (Wang et al., 2006). This method is adapted for binary  
19 or multi-class recognition and is here used for the former (success/failure of the barrier).

20 The basic SVM approach ( $M_{SVM}$ ) consists of defining, in a space of input parameters, the  
21 optimal hyper-plane separating the regions associated with the different classes (success/failure  
22 of the barrier in this context). For that purpose, among all points of the space only those that  
23 are closest to the hyperplane, called support vector, are considered. The optimal hyperplane is  
24 defined as the hyperplane whose margin, i.e. distance from these closest points is maximal. It  
25 is thus calculated by maximizing the distance from the hyperplane to the closest points on each  
26 side.

27 The optimal definition of the hyperplane can require non linear transformation of the data to  
28 another space of potentially higher dimension using kernel functions (Baudat and Anouar, 2001).

29 In this study, the space of the input parameters corresponds to the different parameters as-  
30 sociated with the impact conditions. Linear and radial kernels have been used to build accurate  
31 meta-models (function *svm* in R (V 3.2.3) package *e1071*).

### 1 3.2. Kriging

2 The Kriging (Gaussian process modeling) approach is a procedure of interpolation which is  
3 used in various engineering and applied mathematical problems (Simpson et al., 2001; Sudret,  
4 2012; Zhang et al., 2014). This method is well adapted for approximating results of deterministic  
5 models, such as the post-impact kinetic energy of the block in this study (Martin, 2009). Kriging  
6 models are generally described as the combination of a deterministic component, defined by a  
7 regression model, with a stationary Gaussian process associated with a constant variance and  
8 a correlation function. Contrary to polynomial regression models, Kriging models do not only  
9 assume an underlying global functional form. They can approximate arbitrary functions with  
10 high global and local accuracies.

11 In this study, the meta-model based on a Kriging approach ( $M_K$ ) is developed using the  
12 matlab tool box *UQLab* (Marelli and Sudret, 2014) which enables the creation of an efficient  
13 Kriging predictor based on small number of data. A 3<sup>rd</sup> order polynomial regression model was  
14 used for the deterministic component of the Kriging model. Following recommendations for  
15 a default use in *UQLab* (Marelli and Sudret, 2014), an ellipsoidal Matern function was set as  
16 correlation function.

### 17 3.3. Error quantification

18 The accuracy of the developed meta-models was estimated by comparison with the data  
19 obtained from the FE simulations described and illustrated in Section 2. The prediction error  
20 for both meta-models was estimated using the leave-one-out cross validation method (Allen,  
21 1971).

22 For the SVM approach based meta-model,  $n$  results  $M(x_i)$  from the FEM simulations are con-  
23 sidered. For each parameters combination  $x_i$ , a meta-model is created using all FEM simulation  
24 results except  $M(x_i)$ . The meta-model prediction for  $x_i$  ( $M_{SVM}^i(x_i)$ ) is compared to the remaining  
25 result  $M(x_i)$  observed from the FEM simulations. This comparison is repeated for all  $x_i$  ranging  
26 between  $x_1$  and  $x_n$ . The global accuracy of the meta-model ( $Q(M_{SVM})$ ) is evaluated as follows :

27

$$Q(M_{SVM}) = 1 - \left( \frac{1}{n} \sum_{i=1}^n M(x_i) - M_{SVM}^i(x_i) \right) \quad (1)$$

1 The results of the SVM based meta-model were further discussed with reference to the mis-  
2 classification rate defined as follows. With reference to the FE observations, the SVM based  
3 meta-model can provide bad (false,  $F$ ) or good prediction (true,  $T$ ). As described in Tab. 2, a  
4 false prediction can be positive ( $FP$ ) if a barrier success ( $B_{Succ}$ ) is estimated for a case in which  
5 failure ( $B_{Fail}$ ) was observed; a false prediction can be negative ( $FN$ ) if a barrier failure ( $B_{Fail}$ ) is  
6 estimated for a case in which a success ( $B_{Succ}$ ) was observed. In a similar way, good prediction  
7 can be positive when the barrier success ( $B_{Succ}$ ) is both estimated and observed and negative  
8 when the barrier failure ( $B_{Fail}$ ) is both estimated and observed. Based on these definitions, two  
9 indicators were used to discuss the performance of the SVM based meta-model: the false neg-  
10 ative rate ( $FN_r = \frac{FN}{FN+TP}$ ) and the false positive rate ( $FP_r = \frac{FP}{FP+TN}$ ). In the context of this  
11 study, the false positive rate ( $FP_r = \frac{FP}{FP+TN}$ ) is the most relevant to deal with as it focuses on the  
12 most critical situation. In fact, a high  $FP_r$  value is associated to an overestimation of the barrier  
13 capacity by the meta-model, with the meta-model erring on the unconservative side.

Table 2: Definition of cases for assessing the meta-models performance

	SVM prediction	
FE observation	$B_{Fail}$	$B_{Succ}$
$B_{Fail}$	$TN$	$FP$
$B_{Succ}$	$FN$	$TP$

14 For the Kriging approach based meta-model, a similar leave-one-out cross validation method  
15 as for the SVM approach based meta-model was used. The values of the residual block kinetic  
16 energy predicted by the meta-model  $M_{E,K}^i(x_i)$  were compared to those obtained from the FE sim-  
17 ulations ( $M_E(x_i)$ ). The accuracy of the meta-model is evaluated using the mean ( $Mean_{Err}$ ) and  
18 standard deviation ( $Sd_{Err}$ ) of the residual error.  $Mean_{Err}$  was calculated as:

$$Mean_{Err} = \frac{1}{n} \sum_{i=1}^n (M_E(x_i) - M_{E,K}^i(x_i)) \quad (2)$$

19  
20  $Sd_{Err}$  is calculated as:

$$Sd_{Err} = \sqrt{\frac{\sum_{i=1}^n (M_E(x_i) - M_{E,K}^i(x_i))^2}{n} - Mean_{Err}^2} \quad (3)$$



#### 1 4. Meta-models of the cable-net barrier

2 In this section the results of the meta-models of the cable-net barrier described in Section  
 3 2 are illustrated and discussed. The validation of the meta-models was pursued by comparison  
 4 with the data obtained by the FE simulations. Focus is placed on the influence of the parameters  
 5 range on the performance of the considered meta-models.

##### 6 4.1. Wide range based meta-models

7 This section presents and discusses the results from the two meta-models developed based  
 8 on the wide range set FE simulations (*WR*, Tab. 1).

9 Results of the meta-model addressing the ability of the barrier in stopping the block are given  
 10 in Fig. 6 where symbols in grey stand for good prediction by the meta-model compared to FE  
 11 simulations results. Bad predictions are grouped as positive (red) or negative (yellow) according  
 12 to the definition given in Tab. 2. In particular, as described in Tab. 3, the meta-model failed  
 13 to predict 8 out of 26 barrier success ( $FN_r = 32\%$ ) and 5 out of 254 barrier failure ( $FP_r = 2\%$ ).  
 14 Over the 5 misclassified failures of type  $FP$ , 1 was related to mesh perforation, 3 were related  
 15 to global failure and 1 was related to block rolling over the barrier. It can be concluded that the  
 16 barrier efficiency in arresting the block is slightly overestimated as only 2% of the failure cases  
 17 are not predicted by the meta-model. The global accuracy of the meta-model,  $Q(M_{SVM})$ , was  
 18 found equal to 95% according to eq. 1.

Table 3: SVM based meta-model: wide range results

	Prediction		
Observation	$B_{Fail}$	$B_{Succ}$	
$B_{Fail}$	249	5	$FP_r = 2\%$
$B_{Succ}$	9	17	$FN_r = 35\%$

19 The meta-model dealing with the block kinetic energy reduction was created excluding the 26  
 20 simulations in which the block were stopped by the barrier. According to eq. 2 and 3, the mean  
 21 error,  $Mean_{Err}$ , and standard deviation,  $Sd_{Err}$  of the  $M_K$ , are 0.52 kJ and 200 kJ respectively. The  
 22 former value indicates that the meta-model prediction is unbiased, with the practical implication  
 23 that there are as many unconservative predictions than conservative ones. The later value appears  
 24 rather high compared to the barrier nominal capacity.

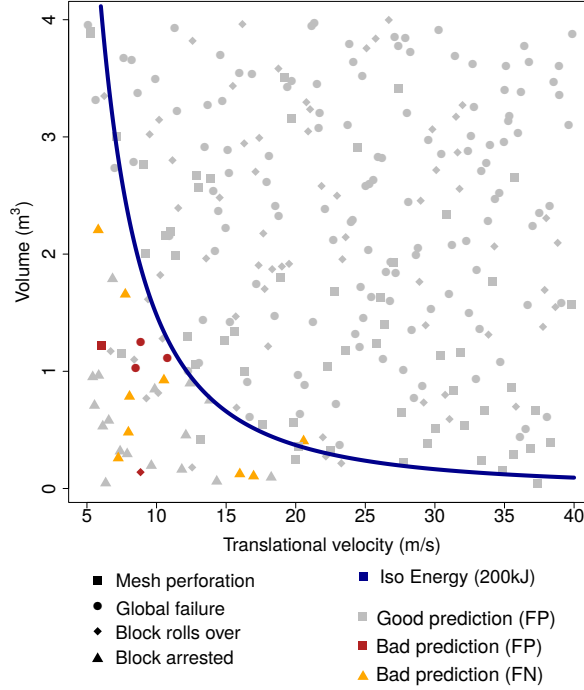


Fig. 6. Prediction of the of  $B_{Succ}$  and  $B_{Fail}$  as a function of the block volume and translational velocity for the wide range scenario.

1        The black curve on Fig. 7 gives the cumulative distribution of the difference between the  
 2 energy reduction observed in the FE simulations ( $M(x_i)$ ) and the corresponding value as predicted  
 3 by the meta-model ( $M_k(x_i)$ ) normalised by the incident block kinetic energy ( $E_{in}$ ). Cases where  
 4 the block kinetic reduction predicted by the meta-model is higher than values observed in the  
 5 FE simulations correspond to negative ratio values, and reveal an error on the unconservative  
 6 side. On the contrary, error on the conservative side consists in cases where the predicted energy  
 7 reduction is less than the observed value, corresponding to positive ratio values. In 5% of the  
 8 cases, the overestimation of the barrier capacity in reducing the block kinetic energy prediction  
 9 by the meta-model exceeds 50 % of the incident block kinetic energy.

10 *4.2. Narrow range based meta-models*

11        The meta-models for the narrow range analysis were created using the second plan of exper-  
 12 iments consisting of 280 combinations of the 6 input parameters (*NR*, Tab. 1).

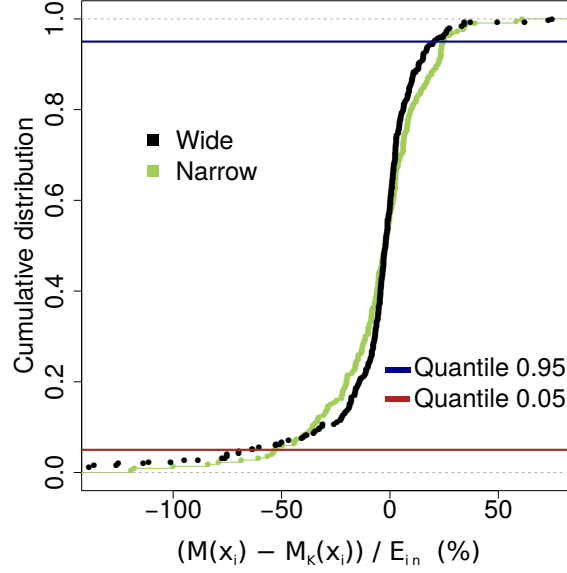


Fig. 7. Cumulative distribution of the ratio between the prediction error ( $M(x_i) - M_k(x_i)$ ) of the block energy reduction after the impact on the barrier and the total incident block kinetic energy  $E_{in}$  for the wide (black) and narrow (green) ranges sets.

1

2 The accuracy of the model dealing with the barrier block arresting ability was evaluated  
 3 according to eq. 1 and resulted in  $M_{SVM}$  equal to 92%. The meta-model failed to predict 16  
 4 barrier success over 61 ( $FN_r = 27\%$ ) and failed to predict 6 barrier failures over 219 ( $FP_r = 3\%$ )  
 5 (Table. 4). Over these 6 misclassified cases, 5 are related to mesh perforation and 1 is related to  
 6 global failure (Fig. 8).

7 Here again, the meta-model overestimates the barrier capacities and 3% of the failure cases are  
 8 not predicted by the meta-model.

Table 4: Quality evaluation for the meta-model created for narrow range values.

Observation	Prediction		
	$B_{Fail}$	$B_{Succ}$	
$B_{Fail}$	213	6	$FP_r = 3\%$
$B_{Succ}$	16	45	$FN_r = 27\%$

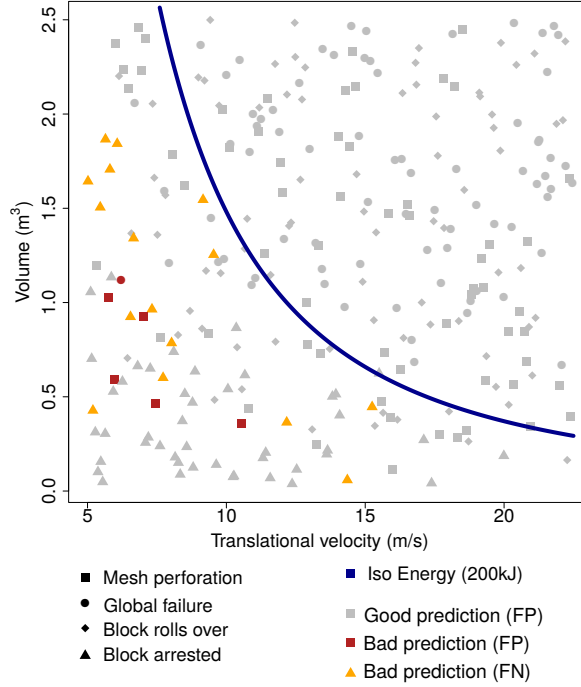


Fig. 8. Prediction of the of  $B_{Succ}$  and  $B_{Fail}$  for the narrow range scenario. Good and bad predictions are indicated by grey and red symbols receptively. The shape of the symbols indicate the mode of failure.

1 As for the meta-model concerning the block kinetic energy reduction, the mean error,  $Mean_{Err}$   
 2 , and standard deviation,  $Sd_{Err}$ , of the  $M_K$  are  $-5.21 \text{ kJ}$  and  $111 \text{ kJ}$  respectively. The same com-  
 3 ments as for the wide range results hold. Nevertheless, the lower standard deviation indicates that  
 4 this meta-model is more efficient in predicting the block kinetic energy reduction.

## 5. Discussion

6 The aim of this article being to propose using meta-models for assessing rockfall protection  
 7 barriers efficiency, this section compares the two approaches (WR and NR) and discusses the  
 8 advantages over classical design approaches in using meta-models.

### 9 5.1. Influence of the range considered

10 The meta-models have been developed considering two ranges of values for the input param-  
 11 eters. Intuitively, a meta-model developed for a range of input parameters fitted to the barrier

1 nominal capacity is expected to provide much better results.

2        Similar trends in terms of model quality are observed for both meta-models and the difference  
3 between meta-models developed for narrow and large ranges is not that pronounced. As for the  
4  $M_{SVM}$  almost the same global accuracy is obtained for wide and narrow ranges (92/95.3%). A  
5 significantly smaller  $FP_r$  rate is observed for the narrow range (27/32 %). In addition, the model  
6 developed for the narrow range accounts for a larger number of arrested blocks over the 300  
7 simulations. Its ability in detecting success cases is thought to be higher.

8        As for the the prediction of the block kinetic energy reduction, both models have a  $Mean_{Err}$   
9 around 0  $kJ$ . However, the predictions  $M_K$  are significantly more accurate for the narrow range  
10 compared to that for the wide range. Indeed, the error standard deviation of the meta-model  
11 based on the narrow range is almost half that of the meta-model based on the wide range (111  $kJ$   
12 compared to 200  $kJ$ ).

13

14        In the end, the difference between the two meta-models appear rather small, the narrow range  
15 resulting in a slightly more accurate meta-model. Results obtained using the narrow range are  
16 considered in the following section.

## 17 5.2. Benefits of the meta-models

18        The current design practices are mainly based on the barrier nominal capacity. In this study,  
19 the nominal capacity was considered as the reference value obtained from impacts following the  
20 recommendations of the European guideline ETAG 027 (EOTA, 2013). A straightforward design  
21 for this specific barrier would consider that all the block having a kinetic energy less than 200  $kJ$   
22 are stopped. Similarly, the block kinetic energy reduction by this barrier would be computed as  
23 the block incident kinetic energy minus 200  $kJ$ .

24        As for the efficiency of the barrier in arresting the block, results presented in section 2 have  
25 shown the limits of an assessment based on the barrier nominal capacity, while section 4 has  
26 suggested the interest of meta-models. A detailed analysis of the results presented in Figure 8  
27 shows that the prediction by the meta-models below the the iso-kinetic energy line results in  
28 4.8% of False Positive cases while considering the barrier nominal capacity as a criterion led  
29 to a value of 52% (see Figure 3). Restricting the comparison to a block size of 0.7m, leads to  
30 values of 4.54% for the meta-model compared to 33.7 % for the barrier nominal capacity based  
31 approach. This means that the later is far too optimistic with respect to the ability of the barrier

1 in stopping the blocks and that the later is more realistic, demonstrating the benefit in using this  
2 meta-model for design or hazard assessment purpose.

3 As for the kinetic energy reduction, Figure 9 compares estimates based on the barrier nominal  
4 capacity and that from the meta-model. The former is obtained subtracting  $200\text{ kJ}$  to the  
5 block total incident kinetic energy. The full curve is not shown as for large kinetic energies no  
6 difference is observed from one curve to the other. Negative block output kinetic energies results  
7 from the fact that in some cases the block incident kinetic energy is less than the barrier nominal  
8 capacity. These cases are accounted for in the figure but should be neutralised setting the kinetic  
9 energy to zero. The same comment holds for results from the meta-model. This figure shows  
10 that the meta-model  $M_K$  fits rather well with the simulation results (in green). On the contrary,  
11 results based on the barrier nominal capacity shows important difference with the simulation re-  
12 sults, between 0 and  $150\text{ kJ}$ . In fact, the kinetic energy reduction is overestimated when using  
13 the barrier nominal capacity. The overestimation by the meta-model is much less and is limited  
14 to the 0- $50\text{ kJ}$  range. Beyond  $200\text{ kJ}$ , the two approaches are similar.

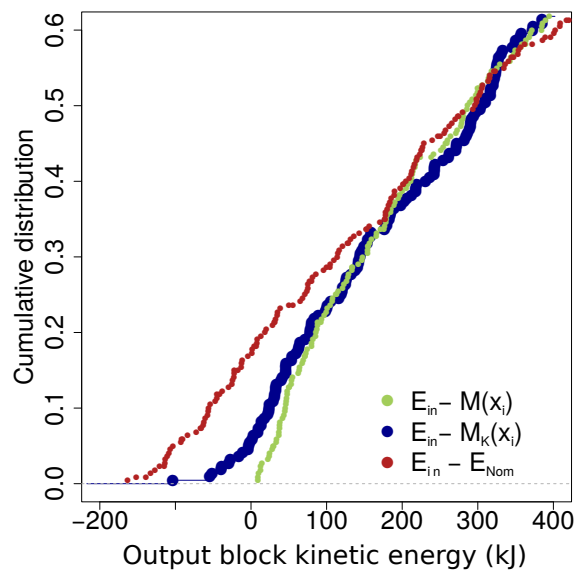


Fig. 9. Comparison between the cumulative distribution of the output kinetic energy predicted by the FE model ( $E_{in} - M(x_i)$  in green), the narrow range meta-model ( $E_{in} - M_K(x_i)$  in blue) and the nominal capacity of the barrier ( $E_{in} - E_{Nom}$  in red).

### 1 5.3. *Towards application to real sites*

2 In the previous section, the benefit in using meta-models has been demonstrated, in particular  
3 by comparison with approaches based on the direct use of the barrier nominal capacity. The  
4 study has shown, that, at least, for the barrier considered, meta-models are much more efficient  
5 in assessing the barrier response.

6 It is worth highlighting that the considered impact conditions did not consider biased trajecto-  
7 ries nor rotational velocities around all block axes. This simplification is thought not to call into  
8 question the conclusions drawn and is assumed to be of negligible influence on the developed  
9 meta-models accuracy.

10 The meta-models were developed considering all the possible impact conditions, and thus  
11 are able to mimic the barrier response whatever the impact case. However, the different impact  
12 scenario within the given parameters ranges were considered equiprobable, which is not realistic.  
13 The impact conditions depend on the block trajectories as observed on real sites. This means that  
14 the statistics in relation to the barrier response that are presented in the previous section, including  
15 the comparison with the barrier nominal capacity, should not be considered for a real site. In lieu  
16 the statistics associated to the ability of the barrier in arresting the blocks for a given site should  
17 be based on the distribution of trajectories of that site. As a consequence, the next steps will  
18 consist in assessing the efficiency of this barrier for a real site. In this aim, the next development  
19 will consist in implementing the meta-models in rockfall trajectory simulation code for a fast and  
20 accurate assessment of the barrier effect on the blocks trajectory.

21 The second meta-model was developed with the aim of evaluating the reduction in kinetic  
22 energy of the block, in case of barrier rupture. Such an event would also result in a change of  
23 the block propagation direction. Implementation of the kinetic energy reduction meta-model in  
24 a rockfall trajectory simulation tool would require making assumptions on the block trajectory  
25 changes after impact. Significant improvement would consist in a meta-model of the block ve-  
26 locity changes, but tackling the problem of building such a meta-model is a very difficult task  
27 because it entails input and output random variables that are statistically dependent. It is a very  
28 difficult problem that was already tackled in 2D for rebound (Bourrier et al., 2009b).

## 1 **6. Conclusion and perspectives**

2 In this article the application of meta-modelling techniques to rockfall protection structures,  
3 focusing on a specific barrier intended for low block kinetic energies has been proposed.

4 The results of 560 FE simulations showed that the barrier efficiency in arresting the block de-  
5 pends not only on the block volume and its translational velocity but it is also controlled by other  
6 parameters related to the block trajectory. As a consequence, quantifying the barrier efficiency  
7 without accounting for their influence may lead to unconservative estimates. For instance, 33.7  
8 % of the impact cases below the nominal barrier capacity, as deduced from a normal-to-the-fence  
9 and centered impact, in fact leads to barrier failure in arresting the block.

10 Two meta-models have been developed, based on the results of the 560 FE simulations: one  
11 concerning the ability of the barrier to arrest the block, the other concerning its ability in re-  
12 ducing the block kinetic energy in case of barrier failure in arresting the block. Two parameters  
13 ranges were considered for creating these two meta-models. The one closer to the barrier nom-  
14 inal capacity appears to be slightly more accurate. Nevertheless, the difference being small,  
15 no optimisation is required with respect to the definition of the ranges for creating a reliable  
16 meta-model. Overall, the meta-models have been shown to provide an accurate prediction of the  
17 barrier response. In particular, the meta-model unconservative error associated to the ability of  
18 the barrier in arresting the block is less than 5%, compared to 33.7 % following a straightforward  
19 design approach. This clearly demonstrates that meta-models represent a promising approach  
20 for improving the design of protective structures, and consequently the rockfall risk mitigation.

21 One possible limitation in the followed methodology is the number of barrier response sim-  
22 ulations required for creating a meta-model. In this case, 280 FE simulations were used. One  
23 perspective to this work would be to reduce the necessary numerical simulations without alter-  
24 ing the meta-model accuracy.

25 The meta-models have been developed with the final aim of quantifying the real efficiency of  
26 the barrier in reducing the hazard or the block kinetic energy downhill. The next step will consist  
27 in introducing the meta-models in rockfall trajectory simulations. This will allow accounting for  
28 the real distributions of the various parameters describing the possible block trajectories and will  
29 represent a significant improvement in quantitative rockfall hazard assessment in presence of a  
30 protective barrier (Corominas et al., 2005).

31 Meta-models may also be used for helping in the optimisation of the design of rockfall barri-



1 ers, allowing for the identification of detrimental mechanisms leading to structure failure. In this  
2 case parameters related to the design of the structures may be considered, such as the position  
3 and initial tension of the cables, post spacing, position of energy dissipating device, if present.  
4 This does represent an inspiring perspective for manufacturers, designers and researchers.

## 5 **References**

- 6 Abaqus (2013). Abaqus Analysis Users Manual. Version 6.11.
- 7 Allen, D. M. (1971). *The Prediction Sum of Squares as a Criterion for Selecting Predictor Variables*. University of  
8 Kentucky.
- 9 Baudat, G. and Anouar, F. (2001). Kernel-based methods and function approximation. volume 2, pages 1244–1249.
- 10 Bertrand, D., Trad, A., Limam, A., and Silvani, C. (2012). Full-Scale Dynamic Analysis of an Innovative Rockfall Fence  
11 Under Impact Using the Discrete Element Method: from the Local Scale to the Structure Scale. *Rock Mechanics and  
12 Rock Engineering*, 45(5):885–900.
- 13 Blatman, G. and Sudret, B. (2010). Efficient computation of global sensitivity indices using sparse polynomial chaos  
14 expansions. *Reliability Engineering & System Safety*, 95(11):1216–1229.
- 15 Bourrier, F., Baroth, J., and Lambert, S. (2015). Accounting for the variability of rock detachment conditions in designing  
16 rockfall protection structures. *Natural Hazards*, 81(1):365–385.
- 17 Bourrier, F., Dorren, L., Nicot, F., Berger, F., and Darve, F. (2009a). Toward objective rockfall trajectory simulation  
18 using a stochastic impact model. *Geomorphology*, 110(3):68–79.
- 19 Bourrier, F., Eckert, N., Nicot, F., and Darve, F. (2009b). Bayesian stochastic modeling of a spherical rock bouncing on  
20 a coarse soil. *Nat. Hazards Earth Syst. Sci.*, 9(3):831–846.
- 21 Brereton, R. G. and Lloyd, G. R. (2010). Support Vector Machines for classification and regression. *Analyst*, 135(2):230–  
22 267.
- 23 Calvetti, F. and Di Prisco, C. (2012). Rockfall impacts on sheltering tunnels: real-scale experiments. *Geotechnique*,  
24 62(10):865–876. WOS:000308697900001.
- 25 Cantarelli, G., Giani, G., Gottardi, G., and Govoni, L. (2008). Modelling rockfall protection fences. In *Proceedings of  
26 the 1st World Landslide Forum*, pages 103–108, Tokyo, Japan.
- 27 Cazzani, A., Mongiov, L., and Frenez, T. (2002). Dynamic finite element analysis of interceptive devices for falling  
28 rocks. *International Journal of Rock Mechanics and Mining Sciences*, 39(3):303–321.
- 29 Chanut, M.-A., Dubois, L., and Nicot, F. (2015). Dynamic Behavior of Rock Fall Protection Net Fences: A Parametric  
30 Study. In *Engineering Geology for Society and Territory - Volume 2*, pages 1863–1867. Springer, Cham. DOI:  
31 10.1007/978-3-319-09057-3\_330.
- 32 Corominas, J., Copons, R., Moya, J., Vilaplana, J. M., Altimir, J., and Amig, J. (2005). Quantitative assessment of the  
33 residual risk in a rockfall protected area. *Landslides*, 2(4):343–357.
- 34 Coulibaly, J. B., Chanut, M., Lambert, S., and Nicot, F. (2017). Nonlinear Discrete Mechanical Model of Steel Rings.  
35 *Journal of Engineering Mechanics*, 143(9).
- 36 de Miranda, S., Gentilini, C., Gottardi, G., Govoni, L., Mentani, A., and Ubertini, F. (2015). Virtual testing of existing  
37 semi-rigid rockfall protection barriers. *Engineering Structures*, 85:83–94.

- 1 de Miranda, S., Gentilini, C., Gottardi, G., Govoni, L., and Ubertini, F. (2010). A simple model to simulate the full-  
2 scale behaviour of falling rock protection barriers. In *Proceedings of the 7th International Conference on Physical*  
3 *Modelling in Geotechnics-ICPMG*, volume 2, pages 103–108, Tokyo, Japan.
- 4 EOTA (2013). ETAG 027 : Guideline for European Technical Approval of Falling Rock Protection Kits.
- 5 Escallòn, J. P., Wendeler, C., Chatzi, E., and Bartelt, P. (2014). Parameter identification of rockfall protection barrier  
6 components through an inverse formulation. *Engineering Structures*, 77:1–16.
- 7 Fang, K.-T., Li, R., and Sudjianto, A. (2005). *Design and Modeling for Computer Experiments*. Chapman and Hall/CRC,  
8 Boca Raton, FL.
- 9 Farhang-mehr, A. and Azarm, S. (2005). Bayesian meta-modeling of engineering design simulations: a sequential  
10 approach with adaptation to irregularities. *International Journal for Numerical Methods in Engineering*.
- 11 Gentilini, C., Gottardi, G., Govoni, L., Mentani, A., and Ubertini, F. (2013). Design of falling rock protection barriers  
12 using numerical models. *Engineering Structures*, 50:96–106.
- 13 Gentilini, C., Govoni, L., de Miranda, S. d., Gottardi, G., and Ubertini, F. (2012). Three-dimensional numerical modelling  
14 of falling rock protection barriers. *Computers and Geotechnics*, Complete(44):58–72.
- 15 Gonzalez-Perez, C. and Henderson-Sellers, B. (2008). *Metamodelling for Software Engineering*. Wiley Publishing.
- 16 Gottardi, G. and Govoni, L. (2010). Full-scale Modelling of Falling Rock Protection Barriers. *Rock Mechanics and Rock*  
17 *Engineering*, 43(3):261–274.
- 18 Jin, R., Chen, W., and Simpson, T. W. (2001). Comparative studies of metamodelling techniques under multiple mod-  
19 elling criteria. *Structural and Multidisciplinary Optimization*, 23(1):1–13.
- 20 Kausar, N., Samir, B. B., Abdullah, A., Ahmad, I., and Hussain, M. (2011). A Review of Classification Approaches  
21 Using Support Vector Machine in Intrusion Detection. In *Informatics Engineering and Information Science*, pages  
22 24–34. Springer, Berlin, Heidelberg.
- 23 Kleijnen, J. P. C. (2009). Kriging metamodelling in simulation: A review. *European Journal of Operational Research*,  
24 192(3):707–716.
- 25 Lambert, S. and Bourrier, F. (2013). Design of rockfall protection embankments: A review. *Engineering Geology*,  
26 154:77–88.
- 27 Lambert, S., Bourrier, F., and Toe, D. (2013). Improving three-dimensional rockfall trajectory simulation codes for  
28 assessing the efficiency of protective embankments. *International journal of rock mechanics & mining sciences*,  
29 60:26–36.
- 30 Lambert, S., Gotteland, P., and Nicot, F. (2009). Experimental study of the impact response of geocells as components  
31 of rockfall protection embankments. *Nat. Hazards Earth Syst. Sci.*, 9(2):459–467.
- 32 Ma, Y. and Ding, X. (2002). Face Detection Based on Cost-Sensitive Support Vector Machines. In *Pattern Recognition*  
33 *with Support Vector Machines*, pages 260–267. Springer, Berlin, Heidelberg. DOI: 10.1007/3-540-45665-1\_20.
- 34 Marelli, S. and Sudret, B. (2014). UQLab: A Framework for Uncertainty Quantification in Matlab. In *Vulnerability,*  
35 *Uncertainty, and Risk*, pages 2554–2563. American Society of Civil Engineers.
- 36 Martin, J. D. (2009). Computational Improvements to Estimating Kriging Metamodel Parameters. *Journal of Mechanical*  
37 *Design*, 131(8):084501–084501–7.
- 38 Mentani, A., Giacomini, A., Buzzi, O., Govoni, L., Gottardi, G., and Fityus, S. (2015). Numerical Modelling of a Low-  
39 Energy Rockfall Barrier: New Insight into the Bullet Effect. *Rock Mechanics and Rock Engineering*, 49(4):1247–

1 1262.

2 Mentani, A., Govoni, L., Gottardi, G., Lambert, S., Bourrier, F., and Toe, D. (2016). A New Approach to Evaluate the  
3 Effectiveness of Rockfall Barriers. *Procedia Engineering*, 158:398–403.

4 Mollon, G., Dias, D., and Soubra, A. (2011). Probabilistic Analysis of Pressurized Tunnels against Face Stability Using  
5 Collocation-Based Stochastic Response Surface Method. *Journal of Geotechnical and Geoenvironmental Engineering*,  
6 137(4):385–397.

7 Mountrakis, G., Im, J., and Ogole, C. (2011). Support vector machines in remote sensing: A review. *ISPRS Journal of*  
8 *Photogrammetry and Remote Sensing*, 66(3):247–259.

9 Nicot, F., Cambou, B., and Mazzoleni, G. (2001). From a constitutive modelling of metallic rings to the design of rockfall  
10 restraining nets. *International Journal for Numerical and Analytical Methods in Geomechanics*, 25(1):49–70.

11 Sacks, J., Welch, W. J., Mitchell, T. J., and Wynn, H. P. (1989). Design and Analysis of Computer Experiments. *Statistical*  
12 *Science*, 4(4):409–423.

13 Simpson, T. W., Mauery, T. M., Korte, J. J., and Mistree, F. (2001). Kriging Models for Global Approximation in  
14 Simulation-Based Multidisciplinary Design Optimization. *AIAA Journal*, 39(12):2233–2241.

15 Sonnenburg, S., Rtsch, G., and Schlkopf, B. (2005). Large Scale Genomic Sequence SVM Classifiers. In *Proceedings*  
16 *of the 22Nd International Conference on Machine Learning, ICML '05*, pages 848–855, New York, NY, USA. ACM.

17 Sudret, B. (2008). Global sensitivity analysis using polynomial chaos expansions. *Reliability Engineering & System*  
18 *Safety*, 93(7):964–979.

19 Sudret, B. (2012). Meta-models for structural reliability and uncertainty quantification. *arXiv:1203.2062 [stat]*. arXiv:  
20 1203.2062.

21 Thoeni, K., Lambert, C., Giacomini, A., and Sloan, S. W. (2013). Discrete modelling of hexagonal wire meshes with a  
22 stochastically distorted contact model. *Computers and Geotechnics*, 49:158–169.

23 Toe, D., Bourrier, F., Olmedo, I., Monnet, J.-M., and Berger, F. (2017). Analysis of the effect of trees on block propagation  
24 using a DEM model: implications for rockfall modelling. *Landslides*, pages 1–12.

25 Vapnik, V. (1995). *The Nature of Statistical Learning Theory*. Springer.

26 Volkwein, A. (2005). Numerical Simulation of Flexible Rockfall Protection Systems. *Computing in Civil Engineering*.

27 Wang, Q., Guan, Y., and Wang, X. (2006). SVM-Based Spam Filter with Active and Online Learning.

28 Zhang, Z., Xu, L., Flores, P., and Lankarani, H. M. (2014). A Kriging Model for Dynamics of Mechanical Systems With  
29 Revolute Joint Clearances. *Journal of Computational and Nonlinear Dynamics*, 9(3):031013–031013–13.